Reprinted from Limnology and Oceanography, volume 45, 2000, pp. 1501-1516. Sunda and Huntsman: Effect of Zn, Mn, and Fe on Cd accumulation in phytoplankton: Implications for oceanic Cd cycling. With permission from the American Society of Limnology and Oceanography.

Limnol. Oceanogr., 45(7), 2000, 1501–1516

Effect of Zn, Mn, and Fe on Cd accumulation in phytoplankton: Implications for oceanic Cd cycling

William G. Sunda and Susan A. Huntsman
NOAA Beaufort Laboratory, Beaufort, North Carolina 28516

Abstract

Cd and phosphate concentrations in seawater are closely related, suggesting that Cd distributions, like those of PO_4, are controlled by algal uptake and regeneration. But the factors that control Cd levels in phytoplankton and their influence on oceanic Cd versus PO_4 relationships are poorly known. We examined the effect of important controlling factors (free ion concentrations of Cd, Zn, and Mn and Fe limitation of growth rate) on Cd accumulation by an oceanic diatom (*Thalassiosira oceanica*). More limited comparative experiments were also conducted with a coastal diatom (*T. weissflogii*) and an oceanic coccolithophore (*Emiliania huxleyi*). Cellular Cd:C ratios increased with increasing Cd ion concentrations and decreasing Zn ion concentrations in all species and with decreasing ionic Mn in the diatoms. The effects of Mn and Zn apparently are related to the uptake of Cd by the cells' Mn and Cd/Co transport systems, which are under negative feedback regulation by cellular Mn and Zn. Cd:C ratios were determined in the oceanic diatom as functions of free ion concentrations of Cd, Zn, and Mn over the oceanic range of these metal ions. The data were combined with estimates of free ion concentrations of these metals in seawater to construct models of Cd:C and Cd:P ratios in oceanic phytoplankton. The modeled Cd:P ratios showed good agreement with slopes of Cd versus P relationships in different oceanic regimes. The models suggest that the high Cd versus phosphate slopes found in iron-depleted waters of the Southern Ocean and subarctic Pacific result from unusually high levels of zinc depletion in these waters. The resulting low zinc ion concentrations induce high levels of Cd uptake by phytoplankton, yielding high algal Cd:P ratios. The heavy depletion of zinc may be linked to elevated Zn:C and Zn:P ratios in iron-limited diatoms, as observed in experiments we conducted with *T. oceanica*.

Cd is usually thought of as a toxic metal, but recent evidence indicates that it can nutritionally substitute for Zn in some key Zn enzymes such as carbonic anhydrase (Price and Morel 1990; Morel et al. 1994; Cullen et al. 1999). Like Zn, Cd is strongly depleted in surface seawater, apparently because of uptake by phytoplankton (Boyle et al. 1976; Bruland et al. 1978). Concentrations of Cd are closely correlated with those of phosphate and nitrate, and, in the central North Pacific, Cd and PO_4 levels both increase by ~500-fold between the surface and 800 m (Bruland 1980).

Correlations between Cd and PO_4 concentrations in seawater have been combined with Cd:Ca ratios in fossil tests of foramanifera to estimate paleooceanic phosphate distributions (Boyle 1988). These, in turn, have yielded insights into relationships between past oceanic circulation patterns and glacial/interglacial climate cycles (Boyle 1988; Elderfield and Rickaby 2000). The Cd versus P relationship used in this analysis is remarkably consistent for most of the ocean but deviates for unknown reasons in certain Fe-limited regions, including the subarctic Pacific (Martin et al. 1989) and the Southern Ocean (Martin et al. 1990*a*; Frew and Hunter 1992).

The close relationship between Cd and PO_4 in the ocean is believed to result from the uptake of both constituents by phytoplankton in surface waters and remineralization at depth, but the factors controlling algal uptake of Cd and resulting cell ratios of Cd to major nutrient elements (C, N, and P) are poorly understood. Previous studies with coastal diatoms have shown that algal Cd concentrations are not only controlled by aqueous Cd ion concentrations but are also inversely related to Mn and Zn ion concentrations (Lee et al. 1995; Sunda and Huntsman 1996, 1998*a*). Enhanced cellular Cd concentrations at low ionic Mn were linked both to uptake of Cd by the cell's Mn uptake system and to reduced biodilution rates associated with Mn limitation of growth rate.

Here we report results of culture experiments in trace-metal ion-buffer systems that investigate the relationship between Cd:C ratios in marine phytoplankton and important controlling variables: free ion concentrations of Cd, Zn, and Mn ($[Cd^{2+}]$, $[Zn^{2+}]$, and $[Mn^{2+}]$). The effect of growth limitation by Fe was also examined because of the enhanced depletion of Cd relative to major nutrients in Fe-limited regions of the ocean. Cellular uptakes of Zn, Co, or Mn were also examined in many of the experiments because of their demonstrated linkages to uptake and utilization of Cd (Price and Morel 1990; Sunda and Huntsman 1998*a*). Three species were investigated, including the coastal diatom, *Thalassiosira weissflogii* (clone Actin), a related oceanic diatom, *T. oceanica* (clone 13-1), and an oceanic coccolithophore, *Emiliania huxleyi* (clone A-1387). The relationships between Cd:C and controlling variables in *T. oceanica* were combined with estimated values for these variables in seawater (based on published data) to construct quantitative models for algal uptake and removal of cadmium in different oceanic regimes. The model predictions are consistent with Cd:PO_4 ratios (and resultant Cd:C ratios) obtained from the slopes of oceanic Cd versus PO_4 relationships via Redfield uptake and regeneration models (Redfield et al. 1963).

Acknowledgments

This research was funded by grants from the Office of Naval Research. We thank Lisa Lowrey and Patrick Griffin for technical assistance. We also thank Kenneth Bruland for use of his unpublished data for Zn complexation in ocean water and for useful comments on an earlier draft of the paper.

Methods

Long-term culture experiments were run in trace metal ion buffer systems with *T. weissflogii, T. oceanica,* and *E. huxleyi* to determine relationships among important controlling variables (free ion concentrations of Cd, Zn, and Mn and growth limitation by Fe) and relevant dependent variables (cellular Cd:C ratios and uptake rates). The methods used were similar to those in previous culture experiments (Sunda and Huntsman 1992, 1995*a*, 1996, 1998*a*).

Axenic cultures of *T. weissflogii* (clone Actin) and *T. oceanica* (clone 13-1) were obtained from the Provasoli-Guillard Center for the Culture of Marine Phytoplankton, Bigelow Laboratory, Maine. The *E. huxleyi* clone (A-1387) was obtained from Larry Brand. The clones were maintained in f/8 medium (Guillard and Ryther 1962) by use of sterile technique until needed. Cells were grown at 20°C and pH 8.2 ± 0.1 in 450-ml polycarbonate bottles containing 250 ml of 36‰ seawater medium. They were grown under fluorescent lighting at an intensity of ~500 μmol quanta m^{-2} s^{-1} on a 14:10 h light:dark cycle.

The experiments were conducted in filtered Gulf Stream seawater enriched with 32 μM $NaNO_3$, 2 μM Na_2HPO_4, 40 μM Na_2SiO_3, 10 nM Na_2SeO_3, 0.074 nM vitamin B_{12}, 0.4 nM biotin, and 60 nM thiamin. Trace-metal ion-buffer systems were added to quantify and control free trace metal ion concentrations. These buffers consisted of 0.1 mM "free" ethylenediamine-tetraacetic acid (EDTA; Ca^- and Mg-EDTA chelates), 40 nM $CuCl_2$, 100 nM $NiCl_2$, and varied concentrations of Cd, Zn, Co, Mn, and Fe. Zn was added with an equivalent concentration of EDTA so that its addition at high concentrations would not alter the free EDTA concentration and thereby alter free ion concentrations of other metals. After preparation, the media were equilibrated for 24 h before cell inoculation.

Free ion concentrations of Zn, Co, Cd, Mn, Cu, and Ni in the media were computed from the total metal concentration and the extent of metal complexation by EDTA and inorganic ions. Total metal concentrations were computed from the sum of the concentration of added metal salt, the estimated background concentration in the seawater, and the measured concentrations of metal added with stock solutions of radiotracers, EDTA, and major nutrients. Background Zn, Co, Cd, Mn, and Fe concentrations were estimated to be 0.9, 0.01, 0.01, 2, and 1 nM, respectively (Sunda and Huntsman 1998*a*). The extent of metal complexation was determined from equilibrium calculations as described in Sunda and Huntsman (1992, 1995*b*). The computed ratios for free metal ion concentrations to total metals were $10^{-3.99}$ for Zn, $10^{-3.63}$ for Co, $10^{-3.78}$ for Cd, and $10^{-1.23}$ M for Mn. The computed free cupric and nickel ion concentrations were $10^{-13.52}$ and $10^{-12.89}$ M, respectively. Iron concentrations were 100 nM (as $FeCl_3$) in most experiments and ~1 nM in one iron-limitation experiment, which generated average concentrations of biologically available dissolved iron hydrolysis species of 250 and ~2.5 pM, respectively (Sunda and Huntsman 1995*b*).

To initiate experiments, cells were transferred from f/8 media to experimental media containing the lowest experimental concentration of the metal (or metals) to be varied. They were acclimated for 7–10 cell generations and then were inoculated into radiolabeled media at biomass levels of 0.1–0.2 μmol of cell carbon per liter of medium. The algae were grown for 9–11 cell generations, during which total cell concentrations and volumes were measured daily with a Coulter multichannel electronic particle counter (Model TA-2 or Multisizer II). Specific growth rates were computed during the exponential phase of growth (Sunda and Huntsman 1992).

Cellular concentrations of Cd, Zn, Mn, and Co were measured with the radiotracers ^{109}Cd, ^{65}Zn, ^{54}Mn, and ^{57}Co as described previously (Sunda and Huntsman 1995*a*, 1996). Measurements were made in exponentially growing cultures, 8–9 cell divisions after inoculation. Cellular metal concentrations were converted to cell metal:carbon ratios by dividing them by carbon:cell volume ratios, measured with ^{14}C in separate cultures (Sunda and Huntsman 1995*a,b*). Filtered cells were acid fumed with HCl before ^{14}C counting to remove inorganic carbon, including any coccoliths in *E. huxleyi* cultures. Average daily cell C:volume ratios were 14, 11, 9, and 16 mol L^{-1} of cell volume, respectively, for Fe-sufficient cultures of *T. pseudonana, T. oceanica, T. weissflogii,* and *E. huxleyi.* In Fe-limited cultures of *T. oceanica,* cellular C:volume ratios were reduced to 7 mol L^{-1} (Sunda and Huntsman 1995*b*). Steady-state metal uptake rates (V_{Me}) were computed by multiplying cellular metal concentrations or metal:carbon ratios by the specific growth rate (μ)

$$V_{Me} = [\text{Cell Metal}]\mu. \quad (1)$$

Results

Cd/Zn matrix experiments at intermediate [Mn^{2+}]—Cd/Zn matrix experiments were conducted over ranges of [Cd^{2+}] ($10^{-13.0}$–$10^{-10.0}$ M) and [Zn^{2+}] ($10^{-12.8}$–$10^{-8.3}$ M), approximating those found in the ocean (Bruland 1989, 1992). [Mn^{2+}] and [Co^{2+}] in these experiments were held constant at $10^{-8.5}$ M and $10^{-11.0}$ M, respectively, values that do not limit growth rate of any of the species.

Zn is a limiting nutrient that can be replaced under some circumstances by Cd (Lee and Morel 1995); higher concentrations of both metals can be toxic. Marked differences were observed between oceanic and coastal species in their growth response to low [Zn^{2+}]. The growth rates of the coastal species *T. weissflogii* was limited at [Zn^{2+}] ≤ $10^{-11.4}$ M, whereas those of the oceanic species were unaffected down to the lowest [Zn^{2+}] (Table 1), consistent with previous findings at similar [Co^{2+}] (Sunda and Huntsman 1992). The highest [Zn^{2+}] ($10^{-8.7}$ and $10^{-8.3}$ M) and [Cd^{2+}] (10^{-10} M) inhibited the growth rate of the coccolithophore (*E. huxleyi*) but had no effect on the growth of *T. oceanica* (Table 1). In *T. weissflogii,* increasing [Cd^{2+}] inhibited growth rate at the lowest [Zn^{2+}] but alleviated a slight Zn limitation at an intermediate [Zn^{2+}] ($10^{-10.4}$ M). Such dual effects of Cd have been reported previously for this species (Lee et al. 1995).

Cellular Cd concentrations in the above experiments increased with increasing [Cd^{2+}] and with decreasing [Zn^{2+}] in all species tested (Figs. 1, 2). The lowest cellular Cd concentrations occurred at the highest [Zn^{2+}], and under these

conditions cellular Cd was simply proportional to $[Cd^{2+}]$ in the medium (Fig. 1). As $[Zn^{2+}]$ was decreased, cellular Cd increased by up to 100-fold in each species. At the higher Cd levels, relationships between cell Cd and $[Cd^{2+}]$ showed progressively decreasing slopes in *T. weissflogii* and, to a lesser degree, in *T. oceanica* and *E. huxleyi.*

Although decreases in $[Zn^{2+}]$ caused similar 100-fold increases in cellular Cd at low $[Cd^{2+}]$, the $[Zn^{2+}]$ range over which this occurred varied among species (Figs. 1, 2). In *T. weissflogii,* the largest relative increase in cellular Cd occurred in the $[Zn^{2+}]$ range $10^{-11.4}$–$10^{-10.4}$ M, similar to results found previously with the related coastal diatom *T. pseudonana* (Sunda and Huntsman 1998*a;* Fig. 2A). By contrast, cellular Cd in *E. huxleyi* increased in inverse proportion to $[Zn^{2+}]$, down to a $[Zn^{2+}]$ of $10^{-10.4}$ M, but was constant at lower free Zn values. Results with *T. oceanica* were intermediate between these two cases.

Effect of variations in $[Zn^{2+}]$ and $[Co^{2+}]$ at constant $[Cd^{2+}]$—In the Cd/Zn matrix experiments, the data often were too widely spaced to discern exact shapes of curves for cellular Cd or Cd uptake rate versus $[Zn^{2+}]$. More detailed experiments with *T. oceanica* conducted at constant low $[Cd^{2+}]$ ($10^{-13.1}$ and $10^{-13.0}$ M) and $[Co^{2+}]$ ($10^{-12.0}$ and $\sim 10^{-13.6}$ M), however, clearly revealed sigmoidal shapes for these curves (Figs. 3, 4A). Uptake rates increased by 80-fold as $[Zn^{2+}]$ was decreased from 10^{-10} to $10^{-11.5}$ M, and rates showed minimal variation above and below this range.

In the experiment run at a $[Cd^{2+}]$ of $10^{-13.1}$ M and $[Co^{2+}]$ of 10^{-12} M, cellular Co and Zn uptake rates were also determined (Fig. 3). The dependence of Co uptake rate on $[Zn^{2+}]$ in this experiment was very similar to that observed for Cd uptake. The greatest increase in uptake of both metals occurred as $[Zn^{2+}]$ was decreased from $10^{-10.5}$ to $10^{-11.5}$ M, in a range where cellular Zn became increasingly depleted toward growth-limiting values (Fig. 3). The similarity in the patterns observed here with *T. oceanica* and previously with *T. pseudonana* (Sunda and Huntsman 1998*a*) suggests that both metals are taken up by a common inducible transport system that is under negative feedback regulation by cellular Zn.

The effect of variations in $[Co^{2+}]$ on Cd uptake was examined in *T. oceanica* at low $[Cd^{2+}]$ and $[Zn^{2+}]$ ($10^{-13.0}$ M for both metals). Increases in $[Co^{2+}]$ decreased Cd uptake rates, but not nearly to the extent that variations in $[Zn^{2+}]$ did (Fig. 4A). Increasing $[Co^{2+}]$ from $10^{-13.0}$ M to $10^{-10.5}$ M caused the Cd uptake rate in *T. oceanica* to decrease by only two-fold, whereas the same variation in $[Zn^{2+}]$ caused a 60-fold decrease in Cd uptake rates (Fig. 4A). At equivalent values of $[Zn^{2+}]$ and $[Co^{2+}]$, the cells contained similar concentration of Zn and Co (Fig. 4B). Thus, uptake rates of Cd are much more sensitive to cellular levels of Zn than those of Co. Co is usually present at much lower concentrations than Zn in seawater (Martin et al. 1989). Because of the lower concentrations of Co and the much lower sensitivity of Cd uptake to $[Co^{2+}]$, it is unlikely that Co would affect Cd concentrations in oceanic diatoms.

Effects of Mn on Cd uptake rates—Increases in $[Mn^{2+}]$ have been found to decrease Cd uptake in *T. pseudonana* as a result of Cd uptake by the Mn transport system (Sunda and Huntsman 1996, 1998*a*). The effect of $[Mn^{2+}]$ on Cd uptake was examined here to determine whether a similar uptake mechanism exists in *T. oceanica.* Our studies included a Cd/Zn matrix experiment conducted at low $[Mn^{2+}]$ ($10^{-9.4}$ M; Fig. 5), and an experiment examining the effect of variations in $[Zn^{2+}]$ on cellular Cd and Mn uptake at low and high $[Mn^{2+}]$ ($10^{-9.3}$ and $10^{-8.0}$ M) and constant $[Cd^{2+}]$ ($10^{-11.0}$ M; Fig. 6). Close agreement was seen in the Cd results at low $[Mn^{2+}]$ for the two experiments in cases where the $[Cd^{2+}]$ and $[Zn^{2+}]$ treatments overlapped (Fig. 6). The lower $[Mn^{2+}]$ values in the experiments ($10^{-9.4}$ – $10^{-9.3}$ M) were designed to fall within the estimated range for oceanic waters of the Pacific, whereas a value of $10^{-8.0}$ M falls within the range for shelf waters (Landing and Bruland 1980; Bruland and Franks 1983).

Lowering the $[Mn^{2+}]$ to $10^{-9.3}$ or $10^{-9.4}$ M in the two experiments had little effect on the growth of *T. oceanica,* in accord with previous findings (Sunda and Huntsman 1986). Growth rate was inhibited at $[Zn^{2+}] > 10^{-8.6}$ M at the low $[Mn^{2+}]$ (Fig. 6A), an effect that did not occur at the higher $[Mn^{2+}]$. The growth inhibition by Zn at low $[Mn^{2+}]$ appears to be linked to a Zn inhibition of Mn uptake and possibly to Zn uptake by the Mn transport system, similar to results found for *T. pseudonana* and *Chlamydomonas* sp. (Sunda and Huntsman 1996, 1998*b*). At low $[Mn^{2+}]$ ($10^{-9.3}$ M), increases in $[Zn^{2+}]$ from $10^{-10.1}$ to $10^{-8.1}$ M decreased cellular Mn by 10-fold, supporting this hypothesis (Fig. 6B). Increases in $[Zn^{2+}]$ within the range $10^{-9.1}$ to $10^{-8.1}$ M resulted in a similar relative inhibition of both Mn and Cd uptake rates (Fig. 6C), consistent with both metals being taken up by the cell's Mn transport system, as found previously for *T. pseudonana* (Sunda and Huntsman 1996) and *Chlorella pyrenoidosa* (Hart et al. 1979). As expected from this hypothesis, increases in $[Mn^{2+}]$ from $10^{-9.3}$ M to $10^{-8.0}$ M decreased cell Cd uptake rates (Fig. 6C).

Cellular Zn—Cellular Zn concentrations and steady-state Zn uptake rates were determined in all three species in the initial Cd/Zn matrix experiments and also in *T. oceanica* in the experiments shown in Figs. 3 and 4B. Cellular Zn was measured because of the strong induction of Cd and Co uptake at low $[Zn^{2+}]$, which may be linked to transport of these metals by the cell's Zn transport system or by a system involved in metabolic replacement of Zn by Co or Cd at growth-limiting cellular Zn levels (Sunda and Huntsman 1995*a;* Lee et al. 1995).

Although Zn appreciably affected cellular Cd concentrations in the initial Cd/Zn matrix experiments, variations in $[Cd^{2+}]$ over the range of 10^{-13}–10^{-10} M (the approximate seawater range; Bruland 1992) had no effect on cellular Zn in either of the diatom species (Table 1). In *E. huxleyi,* increases in $[Cd^{2+}]$ over this range decreased Zn uptake rates by 2.4- to 3.6-fold at $[Zn^{2+}] \leq 10^{-10.4}$ M but had no effect at the highest $[Zn^{2+}]$ ($10^{-9.4}$ M; Table 1).

Curves for cellular Zn and Zn uptake rate versus $[Zn^{2+}]$ determined in the Cd/Zn matrix experiments are shown in Fig. 7, along with previous data for *T. pseudonana.* For *T. weissflogii* and *T. oceanica,* the data given are mean values at the four experimental $[Cd^{2+}]$ values, and for *E. huxleyi*

Table 1. Effect of variations in $[Zn^{2+}]$ and $[Cd^{2+}]$ on cellular Zn:C, Cd:C, and Chl *a*:C ratios; mean cell volume; and specific growth rate (μ).

Species (experiment)	−log $[Zn^{2+}]$	−log $[Cd^{2+}]$	Zn:C*	Cd:C	Chl *a*:C	Cell volume	μ
E. huxleyi							
(111)	12.87	13.01	0.393	1.31	0.245	19.8	1.19
		12.01	0.308	9.77	0.172	17.8	1.18
		11.01	0.239	94.2	0.291	21.0	1.19
		10.01	0.188	335	0.134	17.7	0.99
	11.38	13.01	9.34	0.99	0.227	19.1	1.17
		12.01	6.86	8.22	0.213	20.3	1.15
		11.01	5.71	63.0	0.223	20.3	1.18
		10.01	2.87	177	0.202	23.8	1.05
	10.39	13.0	84.0	1.29	0.308	19.3	1.15
		12.01	67.5	9.57	0.262	20.6	1.19
		11.01	75.9	84.8	0.199	17.7	1.09
		10.01	47.7	334	0.165	NA	0.85
	9.40	13.01	79.9	0.066	0.213	23.4	1.13
		12.01	110	0.836	0.165	21.8	1.15
		11.01	97.3	6.71	0.238	21.2	1.14
		10.01	98.2	57.3	0.225	23.1	1.13
(143a)	8.70	11.97	ND	0.088	0.138	37.0	1.05
		11.00	ND	1.17	0.146	36.0	1.06
		10.00	ND	17.4	0.218	35.2	0.90
	8.30	11.00	ND	0.782	ND	64.9	0.58
		10.00	ND	7.04	ND	66.9	0.60
T. oceanica							
(110)	12.63	12.99	0.175	0.451	0.204	106	1.65
		12.01	0.174	3.23	0.242	103	1.62
		11.01	0.212	14.84	0.241	94	1.56
		10.00	0.246	50.3	0.205	94	1.60
	11.37	13.00	4.08	0.198	0.284	93	1.60
		12.01	3.33	1.37	0.203	103	1.62
		11.00	3.30	8.08	0.245	107	1.64
		10.01	3.00	27.2	0.223	102	1.63
	10.38	12.91	11.4	0.034	0.256	105	1.63
		11.99	11.5	0.266	0.210	102	1.62
		11.00	11.2	2.44	0.254	109	1.63
		10.01	10.4	14.6	0.258	107	1.64
	9.39	12.91	29.7	0.0107	0.253	108	1.60
		12.00	27.2	0.082	0.272	104	1.67
		11.02	27.4	0.800	0.248	103	1.62
		10.01	30.7	7.84	0.289	103	1.60
(143b)	8.70	11.97	ND	0.0447	0.219	84	1.27†
		11.00	ND	0.399	0.225	84	1.32†
		10.00	ND	3.88	0.203	85	1.29†
	8.30	11.00	ND	0.280	0.214	85	1.25
		10.00	ND	2.77	0.231	83	1.27
T. weissflogii							
(112)	12.58	13.00	ND	ND	ND	ND	0.18
	12.59	11.99	ND	ND	ND	ND	0.10
	12.59	11.00	ND	ND	ND	ND	0.03
	12.59	10.01	ND	ND	ND	ND	−0.05
	11.38	13.01	1.75	0.298	0.277	974	0.70
	11.38	12.01	2.16	1.80	0.287	805	0.68
	11.38	11.01	1.44	2.83	0.317	880	0.71
	11.38	10.01	1.78	5.66	0.287	923	0.67
	10.39	13.01	9.64	0.0080	0.297	877	0.74
	10.40	12.01	9.17	0.074	0.296	881	0.75
	10.39	11.01	10.9	0.620	0.311	886	0.82
	10.38	10.00	14.5	2.71	0.307	928	0.84
	9.39	13.02	20.4	0.0045	ND	927	0.83
	9.38	11.99	22.0	0.049	0.336	850	0.74

Table 1. Continued.

Species (experiment)	−log $[Zn^{2+}]$	−log $[Cd^{2+}]$	Zn:C*	Cd:C	Chl *a*:C	Cell volume	μ
	9.40	11.01	23.2	0.41	0.324	849	0.77
	9.39	10.00	22.4	2.75	0.316	864	0.75
(143b)	8.70	11.98	ND	0.0218	0.286	938	0.84
	8.70	11.00	ND	0.193	0.339	937	0.87
	8.70	10.00	ND	1.83	0.329	941	0.80

NA, not applicable; ND, not done.

* Units: Zn:C and Cd:C (μmol mol^{-1}), Chl *a* 3:C (mmol mol^{-1}); volume per cell (μm^3), specific growth rate (d^{-1}).

† The decrease in growth rate observed in Experiment 143b relative to that in Experiment 110 is not due to Zn inhibition; rather it is due to the well-documented, but poorly understood, long-term variability in maximum growth rates of diatoms (Brand et al. 1981; Sunda and Huntsman 1986).

only data at the lowest $[Cd^{2+}]$ are plotted. As with relationships for Cd and Co uptake versus $[Zn^{2+}]$ (Fig. 2; Sunda and Huntsman 1995*a*), distinct differences were observed in the Zn uptake curves between the diatoms and the coccolithophore. In agreement with previous studies (Sunda and Huntsman 1992, 1995*a*), Zn uptake rates in all species were proportional to $[Zn^{2+}]$ and approached diffusion-limited values at low $[Zn^{2+}]$. The region where this occurred, however, extended to higher $[Zn^{2+}]$ ($10^{-10.4}$ M) in *E. huxleyi* than in the diatoms (Fig. 7B). Diffusion-limited rates normalized to cell volume are inversely proportional to the square of the cell diameter (Pasciak and Gavis 1974; Hudson and Morel 1993). Accordingly, at low $[Zn^{2+}]$ ($10^{-11.4}$ M), the smallest species, *E. huxleyi* (3.3 μm cell diameter), had a 16-fold higher uptake rate per unit of cell volume than the largest species, *T. weissflogii* (12-μm diameter; Fig. 7B). Cellular Zn concentrations exhibited a smaller (nine-fold) difference among the species because *T. weissflogii* had a 40% lower growth rate than *E. huxleyi*, and cellular metal concentration is inversely related to specific growth rate (Eq. 1). Differences in cellular Zn:C ratios were smaller yet (five-fold) because *T. weissflogii* had a 44% lower cell C:volume ratio than the coccolithophore (Fig. 7A). The large diatom's lower Zn:C cellular ratios at low $[Zn^{2+}]$ should make it more susceptible to zinc limitation.

For *E. huxleyi*, cellular Zn:C showed an abrupt transition to a constant maximum value at $[Zn^{2+}] > 10^{-10.4}$ M. For the diatoms, relationships between cellular Zn:C and $[Zn^{2+}]$ were sigmoidal, with minimum slopes within the $[Zn^{2+}]$ range $10^{-10.5}$–$10^{-9.5}$ M. Within this $[Zn^{2+}]$ range, all three diatoms had virtually identical Zn:C ratios of 10–20 μmol (mol C)$^{-1}$], 13%–30% of the plateau value found in *E. huxleyi*. The Zn data reported here agree well with those in our previous studies (Sunda and Huntsman 1992, 1995*a*).

Effect of Fe limitation on cellular Zn:C and Cd:C—An experiment was conducted at low $[Cd^{2+}]$, $[Co^{2+}]$, and $[Mn^{2+}]$ ($10^{-13.0}$, $10^{-13.0}$, and $10^{-9.6}$ M, respectively); at varying $[Zn^{2+}]$; and at high and low Fe, to determine the effect of Fe limitation on cellular Zn:C and Cd:C ratios in *T. ocean-*

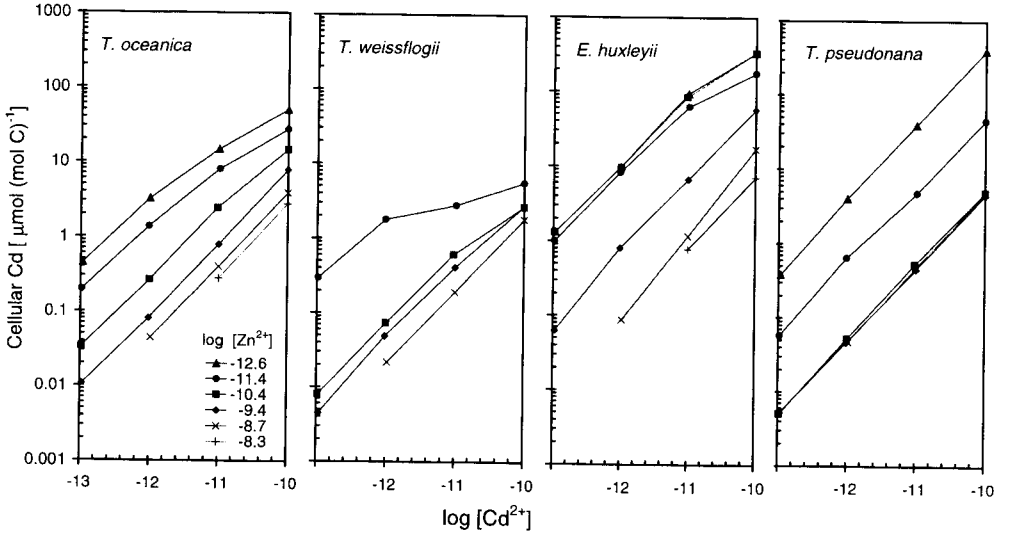

Fig. 1. Log-log relationships between cellular Cd:C and $[Cd^{2+}]$ in *T. oceanica*, *T. weissflogii*, *E. huxleyi*, and *T. pseudonana* at $[Zn^{2+}]$ of $10^{-12.9}$–$10^{-12.3}$ M (▲, see Table 1 for exact values for first three species), $10^{-11.4}$ M (●), $10^{-10.4}$ M (■), $10^{-9.4}$ M (◆), $10^{-8.7}$ M (×), and $10^{-8.3}$ M (+). Data are for Experiments 110, 111, and 143a,b (Table 1), conducted at a $[Mn^{2+}]$ of $10^{-8.54}$ M and $[Co^{2+}]$ of $10^{-11.03}$ M. Data for *T. pseudonana* are for the same set of conditions and are taken from Sunda and Huntsman (1998*a*). The lowest $[Zn^{2+}]$ in the *T. pseudonana* experiments was $10^{-12.3}$ M.

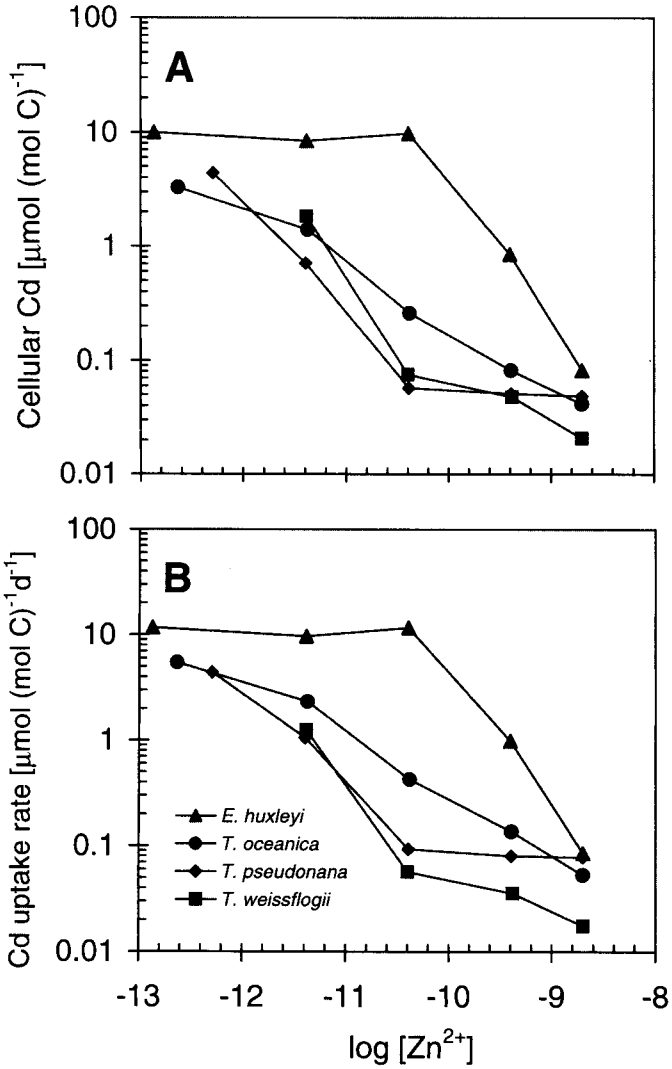

Fig. 2. Log-log relationships between (A) cellular Cd:C and [Zn^{2+}] and (B) steady-state Cd uptake rate and [Zn^{2+}] at a [Cd^{2+}] of 10^{-12} M, [Mn^{2+}] of $10^{-8.54}$ M, and [Co^{2+}] of $10^{-11.03}$ M. Relationships are given for *E. huxleyi, T. oceanica, T. pseudonana,* and *T. weissflogii* for experiments shown in Fig. 1. As in Fig. 1, *T. pseudonana* results are taken from Sunda and Huntsman (1998*a*).

ica. A decrease in total Fe concentration from 100 to 1 nM caused an ~50% reduction in growth rate and an associated 20%–160% increase in Zn:C and Cd:C values. The smallest increase (60% for Zn:C and 20% for Cd:C) was observed at the highest [Zn^{2+}](10^{-10} M), whereas an increase of 160% was observed for both Zn:C and Cd:C at the two lowest free Zn values (Fig. 8A,B).

Discussion

Zn control of cellular Cd and Co uptake—Our results indicate that cellular Cd is controlled by a complex set of variables, including [Cd^{2+}] and [Zn^{2+}] in all species tested, as well as [Mn^{2+}] in diatoms. Fe limitation is also important, but this was examined only in the oceanic diatom. In all

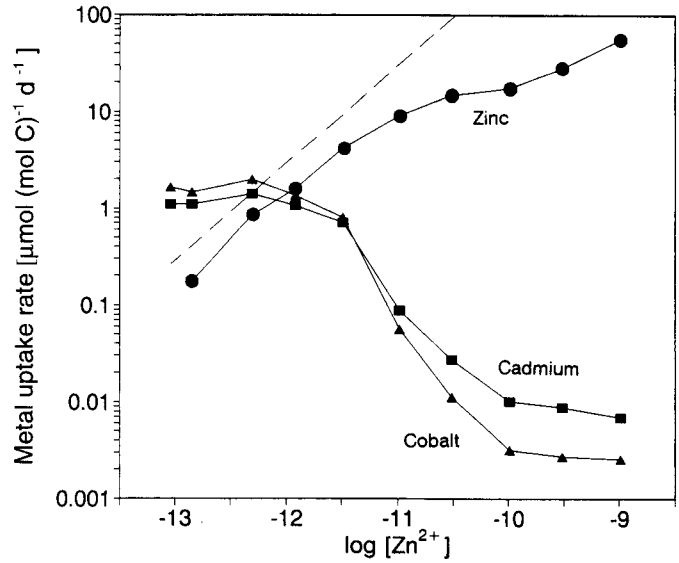

Fig 3. Effect of [Zn^{2+}] on the cellular uptake rates of Zn, Cd, and Co in *T. oceanica* at a [Cd^{2+}] of $10^{-13.1}$ M, [Co^{2+}] of $10^{-12.0}$ M, and [Mn^{2+}] of $10^{-8.5}$ M.. Dashed line gives the limiting rate of Zn uptake permitted by diffusion of labile inorganic Zn species to the cell surface (see Sunda and Huntsman 1995*a*).

species, there is a substantial enhancement in Cd uptake at low [Zn^{2+}]. In *E. huxleyi,* the [Zn^{2+}]-dependent relationships for Cd and Zn uptake are consistent with both metals being taken up by a single inducible transport system that is under negative feedback regulation by cellular Zn (Fig. 9). At [Zn^{2+}] below $10^{-10.4}$ M, Zn-uptake rate is proportional to [Zn^{2+}], consistent with Zn uptake by an undersaturated transport system whose capacity (V_{max}) is constant. But at higher [Zn^{2+}], Zn uptake rates are constant and independent of changes in ionic Zn. In previous experiments with another clone of *E. huxleyi* (BT-6) and other algal species (Sunda and Huntsman 1992; 1998*a,b*), such constancy in Zn uptake rate with increasing [Zn^{2+}] was observed to result first from negative feedback decreases in the capacity (or affinity) of the transport system and then to zinc saturation of the system as [Zn^{2+}] was increased above the half saturation constant (~$10^{-9.6}$ M for clone BT6). Within the region of constant zinc uptake rate (i.e., at [Zn^{2+}] $\geq$ $10^{-10.4}$ M), the uptake rates of other metals transported by the same system should be inversely proportional to [Zn^{2+}] based on theorectical considerations (Sunda and Huntsman 1996). Such behavior is observed in *E. huxleyi* here for uptake of Cd (Fig. 9) and has been observed previously for uptake of Co (Sunda and Huntsman 1995*a*). At a [Cd^{2+}] of 10^{-11} M, linear regressions of log cell Cd uptake rate vs log[Zn^{2+}] within the [Zn^{2+}] range of $10^{-10.4}$–$10^{-8.3}$ M yielded a slope of −1.11 (r^2 = 0.999), close to the theoretically predicted slope of negative unity. Likewise, at an equivalent [Co^{2+}] ($10^{-11.03}$ M) in previous experiments with *E. huxleyi* (Sunda and Huntsman 1995*a*), a regression of log Co uptake rate versus log[Zn^{2+}] over a similar [Zn^{2+}] range ($10^{-10.7}$–$10^{-8.2}$ M) yielded a slope of −0.97 (r^2 = 0.95), again near −1. These results are consistent with all three metals (Zn, Co, and Cd)

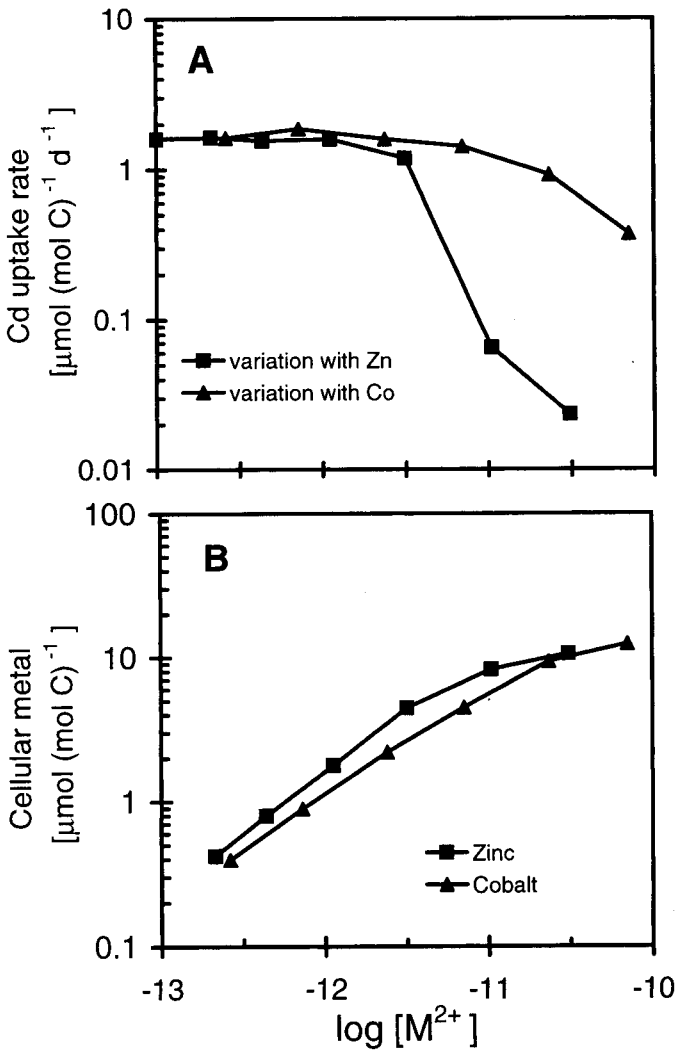

Fig. 4. (A) Cellular Cd uptake rate as a function of $[Zn^{2+}]$ in the absence of added Co (background $[Co^{2+}] \sim 10^{-13.6}$ M) and as a function of $[Co^{2+}]$ in the absence of added Zn ($[Zn^{2+}] \sim 10^{-13}$ M). (B) Cellular Zn : C and Co : C as functions of $[Zn^{2+}]$ and $[Co^{2+}]$, respectively, in the same experiments.

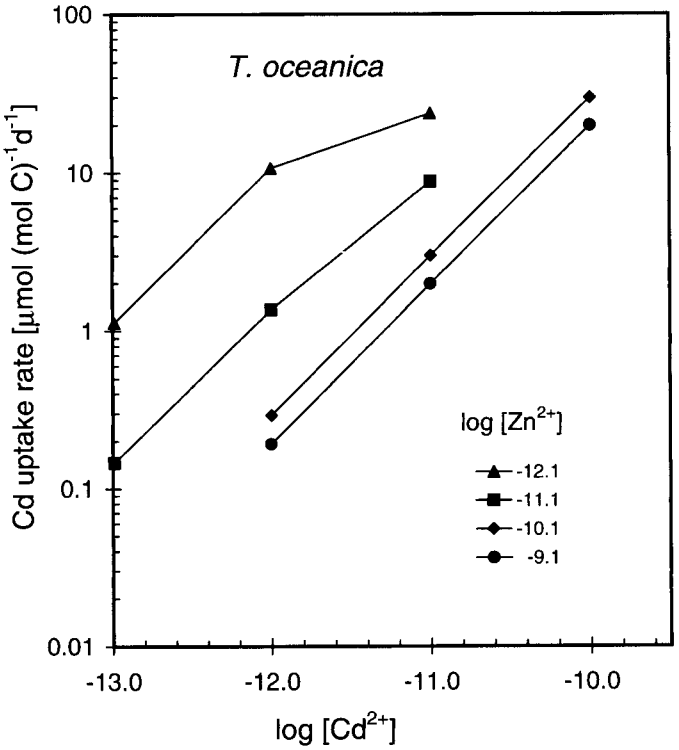

Fig. 5. Log-log plot of steady-state Cd uptake rate in *T. oceanica* vs. $[Cd^{2+}]$ at a $[Mn^{2+}]$ of $10^{-9.4}$ M and $[Zn^{2+}]$ of $10^{-12.09}$, $10^{-11.10}$, $10^{-10.09}$, and $10^{-9.10}$ M. Data are from Experiment 148.

being transported into the cells by a single transport system that is under negative feedback regulation by cellular Zn.

In the diatoms, the $[Zn^{2+}]$-dependent relationships for uptake of Cd, Co, and Zn differ from those in *E. huxleyi,* and the pattern among these relationships is less consistent with there being a single high-affinity uptake system for all three metals. Like *E. huxleyi,* there is a similar pattern of enhanced uptake of Cd and Co at low cellular Zn and $[Zn^{2+}]$, consistent with both metals being taken up by a single inducible transport system. But curves for log Cd and log Co uptake rates versus log$[Zn^{2+}]$ are considerably steeper for the diatoms than for *E. huxleyi,* and, unlike *E. huxleyi,* the steepest portion of these curves occurs in a $[Zn^{2+}]$ range ($\sim 10^{-11.0}$–$10^{-11.5}$ M) well below the region of minimum slope of curves for Zn uptake rate versus $[Zn^{2+}]$ (Figs. 3, 4A). Such Cd and Zn uptake behavior cannot be readily accounted for by both metals being taken up by the same regulated transport system. Thus, although Cd and Co appear to be taken up by a single low-Zn inducible system in the diatoms, Zn may be transported by a separate Zn-regulated uptake system.

The induction of Co and Cd uptake in the diatoms at low $[Zn^{2+}]$ makes sense metabolically, since both metals can biochemically replace Zn in a number of Zn enzymes, including carbonic anhydrase (Morel et al. 1994; Lee et al. 1995; Cullen et al. 1999). As a result, these metals can at least partially alleviate Zn limitation (Price and Morel 1990; Sunda and Huntsman 1995*a*). It is noteworthy in this regard that the $[Zn^{2+}]$ range ($10^{-11.0}$–$10^{-11.5}$ M) where the largest increases in Cd and Co uptake rates occur in the coastal diatoms is also a region where cellular Zn begins to become growth limiting. The difference in uptake patterns for Cd, Co, and Zn between the diatoms and *E. huxleyi* may be related to the different metabolic preferences for these three metals in these algae. The diatoms have a primary requirement for Zn that can be partially met by Co and, to some extent, Cd (Price and Morel 1990; Lee and Morel 1995; Sunda and Huntsman 1995*a*). By contrast, *E. huxleyi* has a primary requirement for Co that can be only partially replaced by Zn, and not at all by Cd (Sunda and Huntsman 1995*a* and unpublished data). In addition, *E. huxleyi* is more susceptible than the diatoms to cadmium toxicity (Table 1).

Cd uptake in diatoms by the Mn transport system—Cd uptake in the diatoms has one additional layer of complexity: uptake by the Mn system at high $[Zn^{2+}]$, where the low-Zn

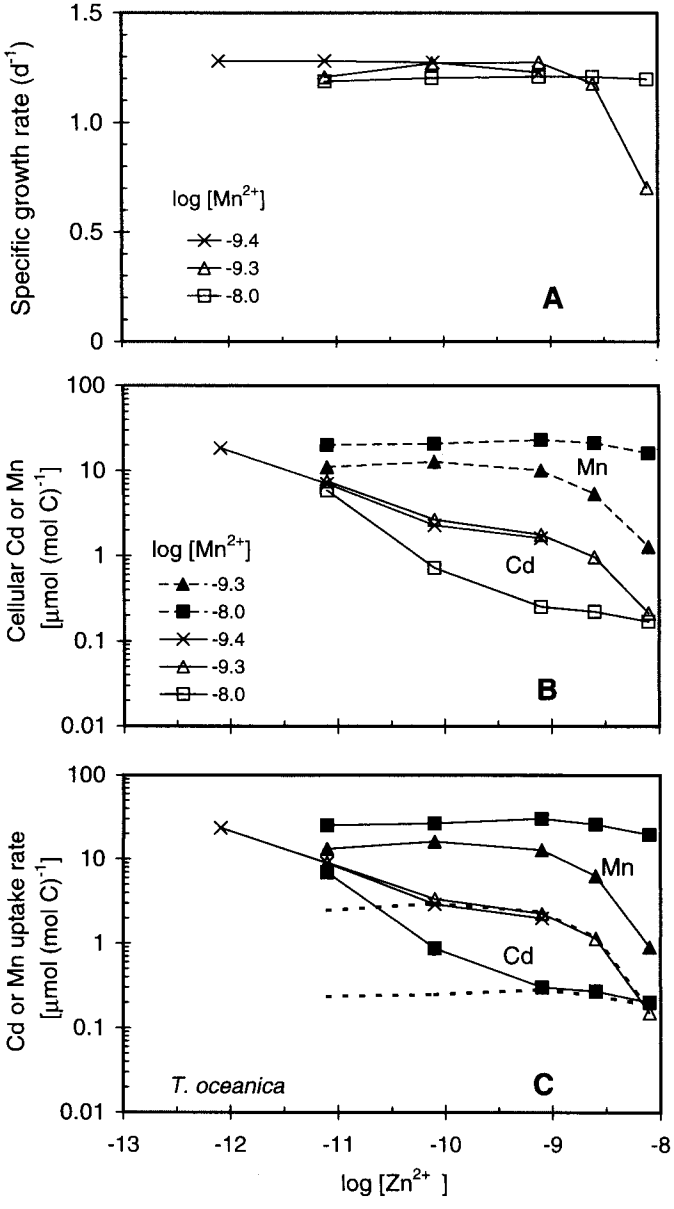

Fig. 6. (A) Specific growth rate, (B) cellular Cd : C and Mn : C, and (C) steady-state uptake rates of Cd and Mn at constant [Cd^{2+}] ($10^{-11.0}$ M) and at low and high [Mn^{2+}]. Open and closed symbols give data for Experiment 191, in which cellular Cd and Mn were measured simultaneously in cultures grown at low and high [Mn^{2+}] ($10^{-9.3}$ and $10^{-8.00}$ M). Cell Cd and growth rate data, measured at a similar low [Mn^{2+}]($10^{-9.4}$ M), are taken from the Cd/Zn matrix experiment (148) shown in Fig. 5. The dotted lines in C give modeled Cd uptake rates computed from Eq. 3, using affinity constants in Table 2 and V_{max} values plotted in Fig. 10 (see Discussion).

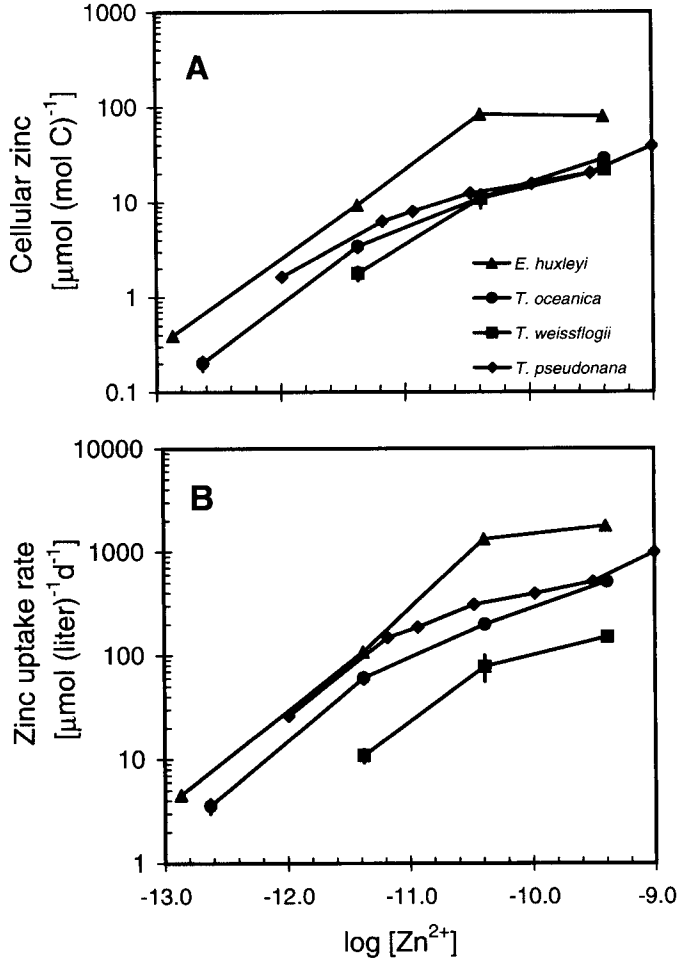

Fig. 7. (A) Log-log relationships between cellular Zn : C and [Zn^{2+}] and (B) between the volume normalized Zn-uptake rate and [Zn^{2+}] for *E. huxleyi, T. oceanica, T. weissflogii,* and *T. pseudonana. E. huxleyi* data are for a [Cd^{2+}] of $10^{-13.0}$ M (Experiment 111, Table 1), whereas those for *T. oceanica* and *T. weissflogii* are average values for [Cd^{2+}] of 10^{-13}, 10^{-12}, 10^{-11}, and 10^{-10} M (Experiments 110 and 112, Table 1). Data for *T. pseudonana* are taken from Sunda and Huntsman (1992), determined in the absence of added Cd ([Cd^{2+}] ~ $10^{-13.8}$ M).

inducible Cd transport system is strongly repressed. Such behavior has been previously described in *T. pseudonana* (Sunda and Huntsman 1996, 1998*a*). As [Zn^{2+}] is increased from 10^{-12} to 10^{-10} M in this species, the Cd uptake rate by the low-Zn inducible system is suppressed by at least 1,000-fold, and Cd is then taken into the cell by the Mn transport system.

The data reported here for *T. oceanica* are also consistent with Cd uptake by the Mn system at high [Zn^{2+}], but differences exist in the uptake behavior between the coastal and oceanic *Thalassiosira* species. The overall Cd uptake rate (V_{Cd}) in either species equals the sum of the rates for the two individual transport systems:

$$V_{Cd} = V_1 + V_2, \quad (2)$$

where V_1 gives the uptake by the Mn system and V_2 gives that for the low-Zn inducible Cd/Co uptake system. Uptake by the Mn system is given by

$$V_1 = \frac{V_{max1}[Cd^{2+}]K_{Cd1}}{[Mn^{2+}]K_{Mn1} + [Cd^{2+}]K_{Cd1} + [Zn^{2+}]K_{Zn1} + 1} \quad (3)$$

Uptake by the Cd/Co system is given by

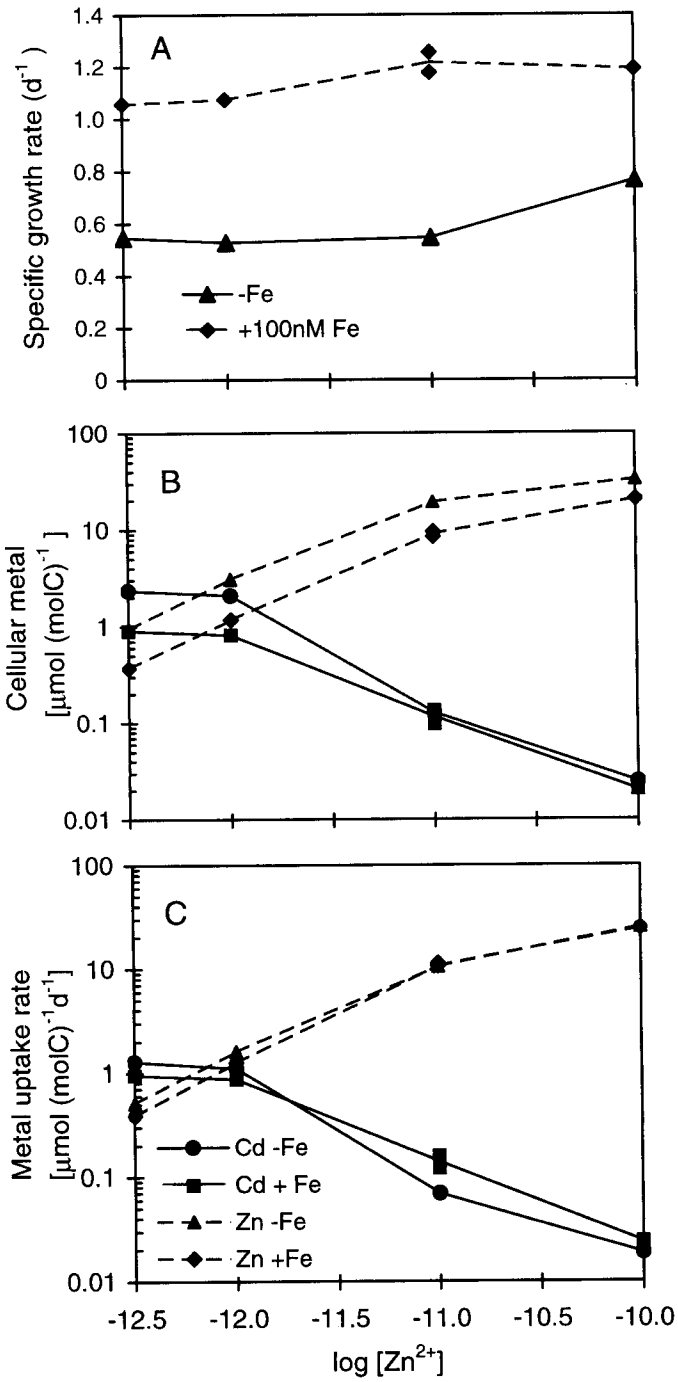

Fig. 8. (A) Specific growth rate; (B) cellular Cd:C and Zn:C, and (C) steady-state cellular Cd and Zn uptake rates in *T. oceanica* as functions of log[Zn^{2+}] under Fe-limiting (~1 nM Fe) and Fe-sufficient (100 nM Fe) conditions. [Cd^{2+}] was maintained at 10^{-13} M, [Co^{2+}] at 10^{-13} M, and [Mn^{2+}] at $10^{-9.6}$ M.

$$V_2 = \frac{V_{max2}[Cd^{2+}]K_{Cd2}}{[Cd^{2+}]K_{Cd2} + [Zn^{2+}]K_{Zn2} + 1} \quad (4)$$

V_{max1} and V_{max2} are the saturation uptake rates for the two systems, and K_{Cd1}, K_{Cd2}, K_{Mn1}, etc., are the steady-state affinity constants for binding of subscripted metals to cell membrane sites for each of the two transport systems.

For the diatoms at low [Mn^{2+}] and high [Zn^{2+}], Cd uptake occurs primarily via the Mn system and is controlled by Eq. 3, as documented for *T. pseudonana* (Sunda and Huntsman 1996). The V_{max} of the Mn system in *T. pseudonana* is under negative feedback regulation and increases by 10-fold as [Mn^{2+}] is decreased from within the vicinity of the half-saturation constant ($10^{-7.1}$ M; the inverse of the affinity constant, K_{Mn1} in Eq. 3) to ~$10^{-8.2}$ M (Sunda and Huntsman 1986). At [Mn^{2+}] below $10^{-8.2}$ M, V_{max} reaches a constant maximum value, and since the transport system is well undersaturated, Cd uptake rates are unaffected by variations in [Mn^{2+}] (Sunda and Huntsman 1998*a*).

A similar pattern of negative feedback regulation of Mn uptake occurs in *T. oceanica* (Sunda and Huntsman 1986). But in this species, K_{Mn1} is seven-fold higher (Table 2), and thus, negative feedback increases in V_{max} occur over a lower [Mn^{2+}] range ($10^{-7.7}$–$10^{-9.0}$ M). Consequently, Mn affects Cd uptake within a lower [Mn^{2+}] range. For example, a decrease in [Mn^{2+}] from $10^{-8.0}$ to $10^{-9.3}$ M caused up to an eight-fold increase in Cd uptake rates in *T. oceanica* (Fig. 6C) but had little effect on Cd uptake in *T. pseudonana* (Sunda and Huntsman 1998*a*).

As done with *T. pseudonana,* we modeled Cd uptake rates at high [Zn^{2+}] in *T. oceanica* from the competitive saturation equation for Cd uptake by the Mn system (Eq. 3) and from estimates of V_{max1}, K_{Cd1}, K_{Mn1}, and K_{Zn1}. This modeling was conducted for the experiment in which we determined both steady-state Cd and Mn uptake rates at constant [Cd^{2+}] (10^{-11} M) and variable [Mn^{2+}] and [Zn^{2+}] (Fig. 6). Estimates of V_{max1} were obtained by assuming that the V_{max} for Cd equals that for Mn, as found for *T. pseudonana* (Sunda and Huntsman 1996). V_{max1} was then computed from the measured steady-state Mn uptake rates (Fig. 6C) and the saturation equation for Mn uptake by the Mn system:

$$V_{Mn} = \frac{V_{max1}[Mn^{2+}]K_{Mn1}}{[Mn^{2+}]K_{Mn1} + [Cd^{2+}]K_{Cd1} + [Zn^{2+}]K_{Zn1} + 1} \quad (5)$$

Rearranging this equation gives

$$V_{max1} = \frac{V_{Mn}([Mn^{2+}]K_{Mn1} + [Zn^{2+}]K_{Zn1} + [Cd^{2+}]K_{Cd1} + 1)}{[Mn^{2+}]K_{Mn1}} \quad (6)$$

Values for V_{max1}, K_{Cd1}, and K_{Zn1} were determined iteratively. Initial values for V_{max1} were computed from Eq. 6 by first ignoring the unknown terms ([Cd^{2+}] K_{Cd1} and [Zn^{2+}] K_{Zn1}) that should be small relative to the other summed terms in the numerator ([Mn^{2+}] K_{Mn1} + 1). Values for K_{Cd1} were then computed from Eq. 3 by use of values for V_{Cd} determined at high [Zn^{2+}] ($10^{-9.1}$–$10^{-8.1}$ M), where Cd uptake by the Mn system should dominate cellular uptake. As before, the unknown term [Zn^{2+}] K_{Zn1} was ignored in this first iteration. The mean computed value of K_{Cd1} was $10^{8.95}$ M^{-1}, 10 times the previously measured K_{Mn1} value ($10^{7.95}$ M^{-1}). This pair of constants is consistent with the equivalent pair for *T. pseudonana,* where K_{Cd1} was also 10 times higher than K_{Mn1} (Table 2). In *T. pseudonana,* K_{Zn1} is 2.5 times K_{Mn1} and one-fourth of K_{Cd1} (Table 2). On the basis of these relative proportions and our K_{Mn1} and K_{Cd1} values in *T. oceanica,* we estimated a K_{Zn1} value of $10^{8.3}$ M^{-1} in the oceanic diatom.

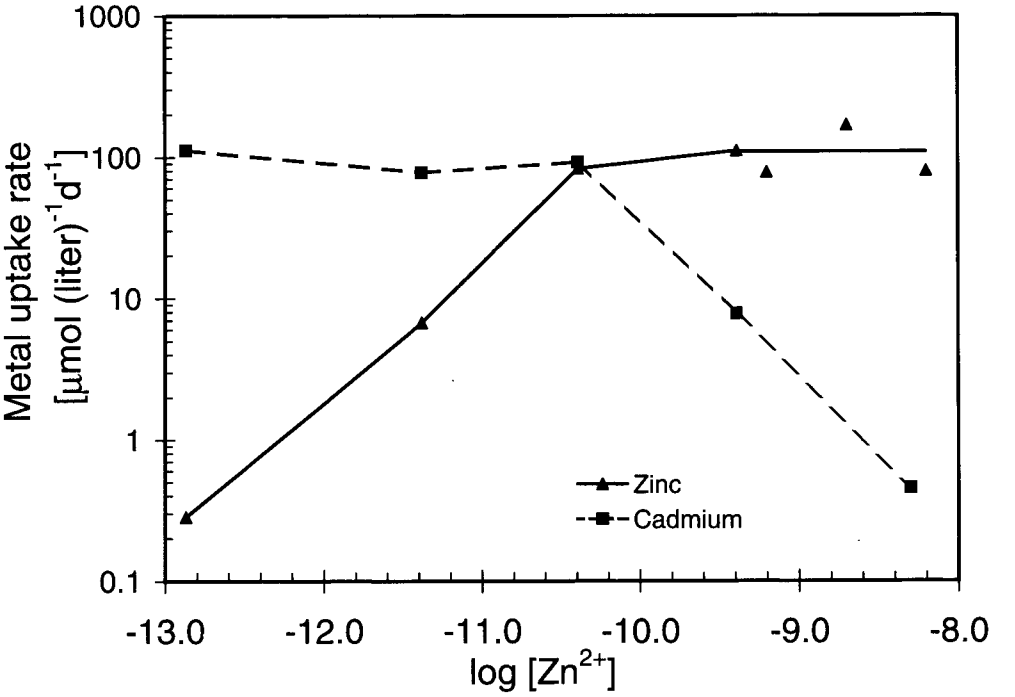

Fig. 9. Log-log plots of Cd and Zn uptake rates vs. $[Zn^{2+}]$ in *E. huxleyi* at a $[Cd^{2+}]$ of 10^{-11} M. Each curve is a mirror image of the other, consistent with both Cd and Zn being taken up by a single regulated transport system.

Using these initial estimates of K_{Cd1} and K_{Zn1}, we recalculated V_{max1} values from Eq. 6 and then obtained new estimates of K_{Cd1} from Eq. 3. The mean of the new K_{Cd1} values is $10^{8.92}$ M^{-1} (Table 2), similar to our initial estimate, indicating that no further model iterations were necessary.

Our final estimates for K_{Cd1}, K_{Mn1}, and K_{Zn1} are listed in Table 2. These values, along with those for V_{max1} (Fig. 10) and for the experimental metal ion concentrations, were inserted into Eq. 3 to compute modeled values for V_{Cd1}. The computed values agree well with our experimental Cd uptake rates for $[Zn^{2+}] \geq 10^{-9.1}$ M (Fig. 6C), supporting the idea that Cd is primarily taken up by the Mn transport system at high $[Zn^{2+}]$ in *T. oceanica.*

Cd uptake by the Mn system is not independent of Zn. In *T. pseudonana,* increasing $[Zn^{2+}]$ begins to depress Cd uptake by this system at $[Zn^{2+}] > 10^{-8.0}$ M, due first to decreases in V_{max} and then to competition for binding to the transport system at $[Zn^{2+}]$ above $10^{-7.5}$ M, the half-saturation constant for Zn binding (Sunda and Huntsman 1996). In *T. oceanica,* the observed decrease in Cd uptake rates at $[Zn^{2+}] > 10^{-9.1}$ M (Fig. 6C) also appears to result from both Zn suppression of V_{max1} (Fig. 10) and from Zn^{2+} competition for binding to the Mn transport system. The Zn suppression of Cd uptake by the Mn system occurs at lower $[Zn^{2+}]$ in *T. oceanica* because of the higher affinity of that system for binding Mn and competing metals (Table 2).

Table 2. Metal-binding affinities for the Mn transport systems in *T. pseudonana* and *T. oceanica.*

	T. pseudonana	*T. oceanica*
log K_{Mn1}	7.1*†	7.95†
log K_{Cd1}	8.1*	8.92 ± 0.04‡
log K_{Zn1}	7.5*	8.3§

* Sunda and Huntsman (1996).
† Sunda and Huntsman (1986).
‡ This study, computed.
§ This study, estimated.

Modeling algal controls on Cd versus P relationships in the ocean—Our results indicate that algal Cd:C ratios in phytoplankton are determined by a number of complex variables, including free ion concentrations of Cd^{2+}, Zn^{2+}, and Mn^{2+} and the individual algal species. In addition, limitation of growth rate by Fe (Fig. 8) or Mn (Sunda and Huntsman 1998*a*) can increase cellular Cd (and Zn) concentrations through metabolic interactions and decreased biodilution rates (*see Eq. 1*). Here we attempt to model algal Cd:C and associated Cd:P ratios that would occur in our oceanic diatom (*T. oceanica*) growing in different oceanic waters to gain insight into biological controls on Cd distributions and Cd versus P relationships in seawater. We have chosen *T. oceanica* for this modeling effort because oceanic diatoms are primarily responsible for the uptake and export of nutrients by phytoplankton in the ocean (Dymond and Lyle 1985). For our modeling effort, we have chosen high-quality data sets from three oceanic regimes, each with differing levels of Fe limitation and differing Cd versus P and Zn versus P relationships: the central North Pacific (Bruland 1980; Landing and Bruland 1980), the subarctic Pacific

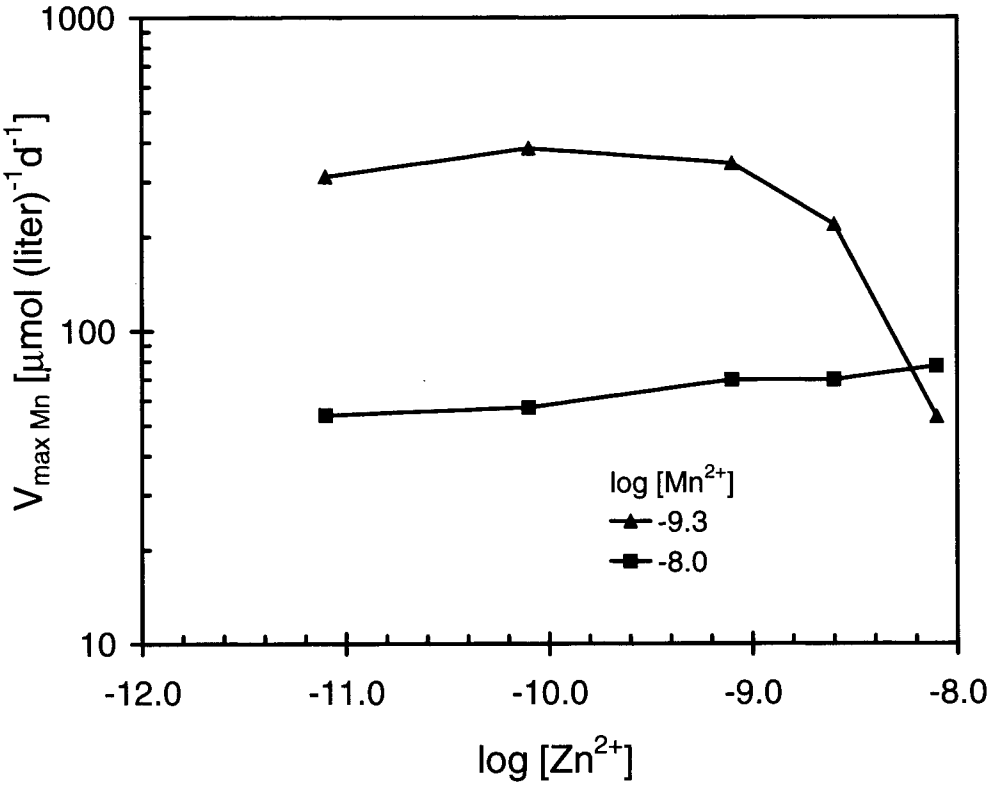

Fig. 10. Log-log plot of V_{max} for the Mn-uptake system in *T. oceanica* vs. [Zn^{2+}] measured at [Mn^{2+}] of $10^{-9.31}$ M and $10^{-8.00}$ M. Values were computed from Eq. 6 using the affinity constants in Table 2 and steady-state Mn-uptake rates from Experiment 191 plotted in Fig. 6C.

(Martin et al. 1989), and the Southern Ocean (Martin et al. 1990*b*) (Fig. 11A,B). In Fig. 11A we have also plotted the Cd versus P relationship in the Indian Ocean (Saagar et al. 1992) because of its similarity to that in the Southern Ocean. This latter relationship was not used in our modeling effort, however, because of the lack of associated high-quality data for dissolved zinc.

According to the ideas of Redfield et al. (1963), major nutrients (N, P, and Si) are depleted in surface ocean waters by algal uptake and are transported to deeper waters by settling of cells and biogenic particles (e.g., fecal pellets). They then are regenerated back into solution by microbial activity. Similar cycles occur for micronutrients (Zn, Cd, Fe, and Cu) as well (Morel and Hudson 1984; Sunda 1994). Such biological uptake, settling, and regeneration cycles combined with thermohaline oceanic circulation results in vertical and horizontal variations in the concentrations of bioactive elements such as P, N, Si, Zn, and Cd. On the basis of Redfield's ideas, the relative changes in Cd and phosphate concentrations between adjacent water parcels should reflect the Cd:P ratios in algae responsible for uptake and vertical transport of these elements provided regeneration rates for Cd and P are similar. Sediment trap data shows that the latter is indeed the case (Knauer and Martin 1981).

Models were constructed to examine the effect of simultaneous variations in [Cd^{2+}], [Zn^{2+}], and [Mn^{2+}] on algal Cd:P ratios in three oceanic regions (Northeast Pacific, subarctic Pacific, and Southern Ocean) with differing Cd versus

Table 3. Regression slopes of Zn vs. P and Si vs. P for the northeast Pacific, subarctic Pacific, and Southern Oceans.

Location	P*	Zn	Zn:P	R^2	Zn:C†	Si:P	R^2	*n*	Reference‡
NE Pacific, Sta. H77 and C1	1.3–3.3	0.8–6	2.51	0.970	24	37.4	0.89	7	1
Subarctic Pacific, Sta. T-5 and T-6	1.1–3.1	1.2–8.8	4.07	0.975	38	50.4	0.963	16	2
Southern Ocean, Drake Passage, Sta. 2	2.1–2.6	1.5–5.1	7.97	0.993	75	97.4	0.994	4	3

* Units: P (µM at 20°C), Zn (nM), Zn:P (mmol mol^{-1}), Zn:C (µmol mol^{-1}), Si:P (mol mol^{-1}).
† Based on the Zn:P slope and the Redfield C:P molar ratio of 106.
‡ References: (1) Bruland 1980; (2) Martin et al. 1989; (3) Martin et al. 1990*b*.

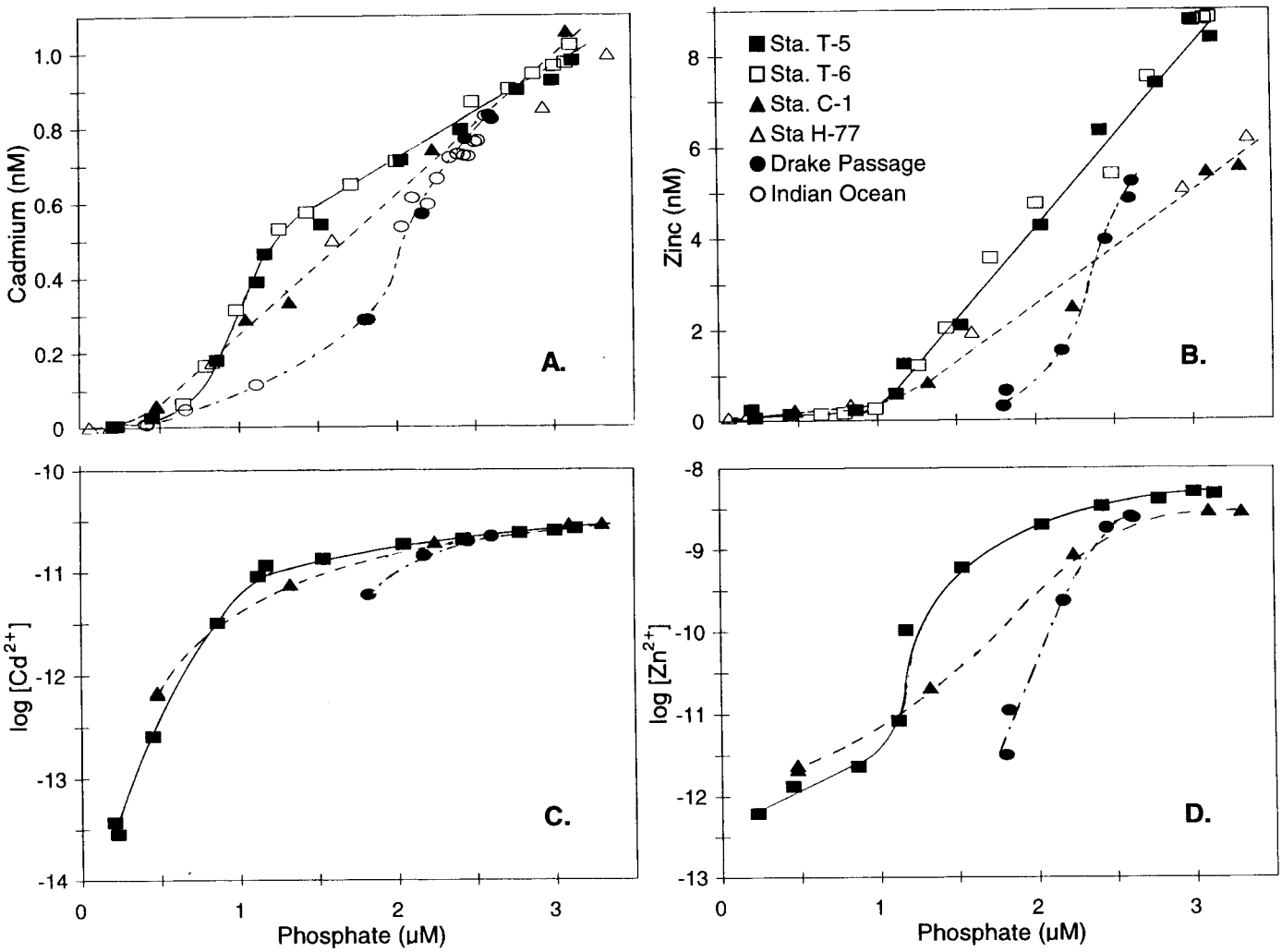

Fig. 11. Dissolved Cd and Zn vs. phosphate and (modeled log[Cd^{2+}] and log[Zn^{2+}] vs. phosphate in the subarctic Pacific (■ Sta. T-5, 39.6°N, 140.8°W, 20–780 m; □ Sta. T-6, 45.0°N, 142.9°W, 20–800 m; Martin et al. 1989), the northeast Pacific (△ Sta. H-77, 32.7°N, 145.0°W, 0–780 m; ▲ Sta. C-1, 37.0°N,124.2°W, 0–750 m; Bruland 1980); Southern Ocean (● Drake Passage, 60.8°S, 63.4°W, 30–400 m; Martin et al. 1990*b*), and Indian Ocean (○ Sta. 5, 14.5°N,67.0°E, 4–1250 m; Saagar et al. 1992).

P and Zn versus P relationships (Fig. 11A,B). We wished to determine the extent to which predicted variations in algal Cd:P ratios could account for observed variations in slopes of Cd versus P plots both within and among the regions.

Variations in [Zn^{2+}] and [Cd^{2+}] in the three oceanic regions (Fig. 11C,D) were computed from speciation models based on published complexation data for the North Pacific (Bruland 1989, 1991) and additional data for the South Pacific and North Atlantic (K. W. Bruland unpubl. data). These data show that up to 99% of the Zn and 70% of Cd in the euphotic zone is complexed by strong chelators present at relatively uniform surface concentrations among the ocean basins so far examined. [Zn^{2+}] was computed from the equation

$$[\text{Dissolved Zn}] = \frac{[Zn^{2+}]}{0.66} + \frac{1.2 \times 10^{-9}[Zn^{2+}]10^{11.0}}{[Zn^{2+}]10^{11.0} + 1} \quad (7)$$

where $10^{11.0}$ M^{-1} is the conditional constant for the binding of Zn by a ligand present at a constant level (1.2×10^{-9} M) down to at depth of at least 400 m (Bruland 1989) and 0.66 is the ratio of [Zn^{2+}] to dissolved inorganic Zn species (Byrne et al. 1988). [Cd^{2+}] was computed from an analogous expression:

$$[\text{Dissolved Cd}] = \frac{[Cd^{2+}]}{0.030} + \frac{1.0 \times 10^{-10}[Cd^{2+}]10^{12.0}}{[Cd^{2+}]10^{12.0} + 1} \quad (8)$$

where 1.0×10^{-10} M is the concentration of the strong organic ligand that binds Cd, $10^{12.0}$ M^{-1} is the conditional stability constant for the complexation of Cd by this ligand (Bruland 1991), and 0.030 is the ratio of [Cd^{2+}] to the concentration of dissolved inorganic Cd species (Byrne et al. 1988). Chelation of Cd was based on data for the mid- to lower euphotic zone, where most export production occurs (Coale and Bruland 1987).

Mn forms only weak complexes with organic ligands, and,

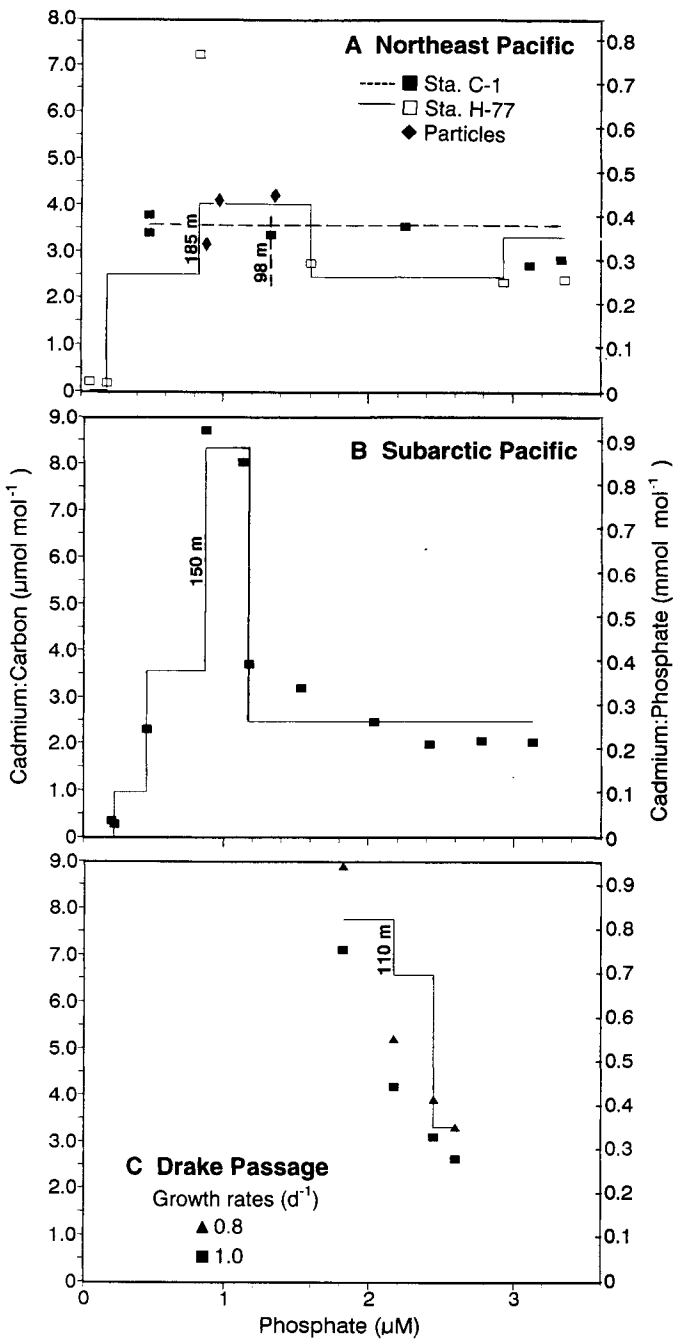

Fig 12. Modeled relationships for Cd:C and Cd:P in an oceanic diatom (*T. oceanica*) growing in water from (A) the northeast Pacific (■ Sta. C-1 and □ Sta. H-77; Bruland 1980), (B) the subarctic Pacific (■ Sta. T-5; Martin et al.1989), and (C) the Drake Passage (Sta. 2, Martin et al. 1990*b*). Drake Passage values were modeled for two specific growth rates: ▲ 0.8 and ■ 1.0 d^{-1}. Modeled Cd:P values agree well with slopes of Cd vs. P relationships (Fig. 11A), which are drawn as solid or dashed lines. The Cd vs. P slopes were computed as point to point values for curvelinear relationships (Sta. H-77, Drake Passage, and Sta. T-5 at $P \leq 1.2$ μM) and by linear regression for linear relationships (Sta. C-I, R^2 = 0.997) or linear portions of curves (Sta. T-5 at $P \geq 1.2$ μM, R^2 = 0.995). Cd:P slopes are given as step functions. Modeled values for the northeast Pacific agree well with Cd:P ratios of suspended particles (◆) taken from the euphotic zone (10–65 m) in that region thus its organic complexation can be ignored. Therefore, $[Mn^{2+}]$ is simply proportional to dissolved Mn:

$$[Mn^{2+}] = 0.72[\text{Dissolved Mn}], \quad (9)$$

where 0.72 is the computed ratio of $[Mn^{2+}]$ to dissolved inorganic Mn species (Byrne et al. 1988). $[Mn^{2+}]$ was computed to be 0.14–0.44 nM in the subarctic Pacific, 0.06–0.2 nM in the Southern Ocean, and 0.19–0.47 nM in the central North Pacific, as based on Eq. 9 and data for dissolved Mn in the three regions taken from Martin et al. (1989, 1990*b*) and Landing and Bruland (1980). The modeling in the preceding section shows that at these low $[Mn^{2+}]$ and at high $[Zn^{2+}]$ ($\geq 10^{-10}$ M), Cd is primarily taken up by the Mn transport system in *T. oceanica* (Fig. 6C). Within the oceanic $[Mn^{2+}]$ range (i.e., at $[Mn^{2+}] < 1.5$ nM), Cd uptake by that system is unaffected by variations in $[Mn^{2+}]$, since the system is well undersaturated and the V_{max} is constant. Thus, the above variations in $[Mn^{2+}]$ in ocean water of 0.06–0.47 nM should not affect Cd uptake by the diatom, simplifying the Cd uptake models. However, as seen from our experiments (Fig. 8), limitation of growth rate by iron increases cellular Cd:C and Zn:C ratios in the oceanic diatom, and these effects need to be taken into account in our models, at least qualitatively.

In our models, measured relationships between Cd uptake rates in *T. oceanica* versus $[Cd^{2+}]$ and $[Zn^{2+}]$ within the oceanic $[Mn^{2+}]$ range (Figs. 5, 6C) were combined with computed relationships between concentrations of the two metal ions and P (Fig. 11C,D) to determine Cd uptake rates (normalized to cell C and P) as functions of phosphate concentration. These rates were divided by specific growth rate (see Eq. 1) to estimate Cd:P and Cd:C algal ratios as functions of phosphate concentration (Fig. 12A–C). In our models, we assumed specific growth rates of 1.1 per day for the northeast Pacific, 1.0 per day for the subarctic Pacific, and 0.8–1.0 per day for the Southern Ocean. The rates are lower than the experimental values (1.2–1.3 per day) and are designed to take into account increases in cellular Cd:C ratios resulting from varying levels of Fe limitation. Evidence exists for a slight Fe limitation in the northeast Pacific (Martin et al. 1989) and for progressively greater limitation in the subarctic Pacific (Martin et al. 1989) and Southern Ocean (Martin et al. 1990*b*).

Modeled $[Cd^{2+}]$ for the northeast and subarctic Pacific decreased by up to 1,000-fold with decreasing P concentration, but the log$[Cd^{2+}]$ versus P relationships for the different oceanic regions were similar (Fig. 11C). Decreases in P were accompanied by even larger (up to 8,000-fold) decreases in $[Zn^{2+}]$, and the relationships between log$[Zn^{2+}]$ and P differed substantially among the regions. At a phosphate concentration of 1.75 μM, the estimated $[Zn^{2+}]$ varied from $10^{-11.5}$ M in the Southern Ocean, where Cd versus P slopes were highest, to $10^{-9.0}$ M in the subarctic Pacific, where slopes were lowest. From our results, such free Zn ion var-

←

(Knauer and Martin 1981). Phosphate values at depths near the bottom of the euphotic zone (98–185 m) are specified to indicate regions where algal growth occurs.

iations should have a major influence on algal Cd:C and Cd:P ratios and, thus, on slopes of Cd versus P relationships.

The modeled algal Cd:P ratios agreed well with the slopes of Cd versus P relationships for the three oceanic regions (Fig. 12A–C). In the northeast Pacific the predicted Cd:P ratios also agreed with those for suspended particulates collected within the euphotic zone (Fig. 12A). Thus, the variation in Cd:P slopes observed at different P concentrations within a given region and that seen at the same P concentration between regions can be accounted for by the predicted variations in the Cd content of our model alga (*T. oceanica*), as controlled by relative variations in $\log[Cd^{2+}]$ and $\log[Zn^{2+}]$. The decrease in Cd:P slopes at P concentrations <0.5 μM (Fig. 11A), the noted "kink" in the Cd versus P relationship found over much of the ocean (Boyle 1988; Frew and Hunter 1992), is explained by large decreases in $\log[Cd^{2+}]$ relative to $\log[Zn^{2+}]$ (Fig. 11C,D).

A sharp maximum in the Cd versus P slope of ~0.8 mmol mol^{-1} is observed in near-surface subarctic Pacific water (20–150 m at Sta. T-6) at phosphate concentrations of 0.6–1.2 μM and in near-surface Southern Ocean water (30–110 m) at phosphate concentrations of 1.8–2.2 μM. The models show that these high slopes can be accounted for by the sharp drop in dissolved Zn relative to phosphate and the resultant large decrease in $\log[Zn^{2+}]$ (Fig. 11B,D), which greatly enhances algal Cd uptake rates. The steepest decline in $\log[Zn^{2+}]$ occurs at a Zn concentration of ~1.2 nM, where the concentration of dissolved Zn drops below that of the strong Zn-binding ligand (Fig. 11B,C). As this occurs, there is a disproportionate increase in the fraction of Zn bound by the strong ligand and an associated sharp decrease in free Zn ion concentrations (Bruland 1989; *see Eq. 7*).

Thus, by controlling Cd uptake rates, variations in Zn concentrations can appreciably influence the slopes of Cd versus P relationships. Ultimately, to understand the factors that control Cd versus P distributions, we must first understand those that control Zn versus P relationships. Like Cd and major nutrients, Zn distributions in the nutricline appear to be controlled by algal uptake and regeneration, as supported by algal uptake models similar to those we report here for Cd (Sunda and Huntsman 1992, 1995*a*). At Zn concentrations of ~1–6 nM, the slope of the Zn versus P relationship in the Southern Ocean (8.0 mmol mol^{-1}) is observed to be twice that (4.1 mmol mol^{-1}) in the subarctic Pacific and about three times that (2.5 mmol mol^{-1}) in the northeast Pacific (Fig. 11B; Table 3). This higher depletion of Zn relative to phosphorus indicates higher Zn:P and Zn:C ratios in the Southern Ocean phytoplankton.

Concentrations of Zn in seawater generally correlate with those of silicate (Bruland 1980), suggesting that algal uptake of the two nutrient elements are somehow linked. Such correlation is also seen in the data sets examined here. Si versus P regression slopes show relative variations among the Southern Ocean, subarctic Pacific, and northeast Pacific similar to the variations discussed above for Zn versus P regression slopes (Table 3). Furthermore, plots of Zn versus Si show a similar proportionality between Zn and silicate concentrations in the three regions (Fig. 13), despite the highly variable Zn versus P and Si versus P slopes within

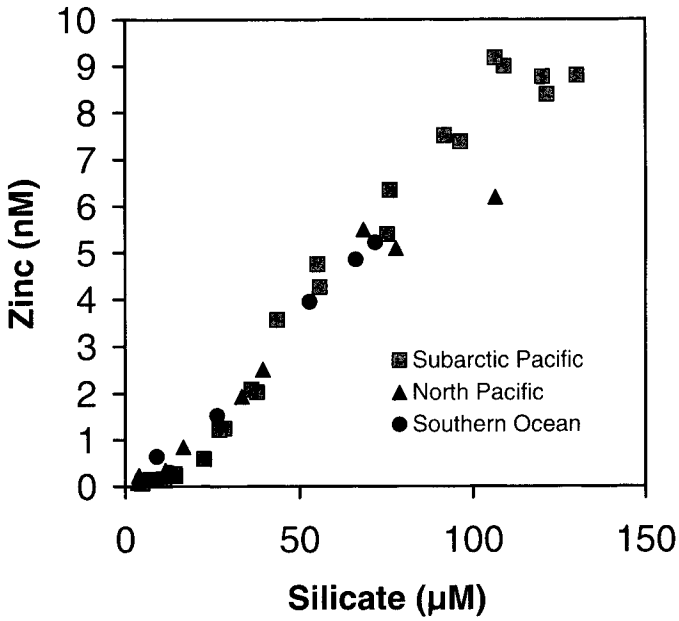

Fig. 13. Relationship between concentrations of dissolved Zn and Si in the subarctic Pacific (Sta. T-5 and T-6, 20–800 m; Martin et al. 1989), the northeast Pacific (Sta. H-77 and C-1, 0–780 m; Bruland 1980), and the Southern Ocean (Drake Passage, 30–400 m; Martin et al. 1990*b*).

and among these regions. From recent at-sea experiments, Fe limitation has been shown to increase the Si:P and Si:N ratios in diatoms by up to three-fold (Hutchins and Bruland 1998; Takeda 1998). This effect in turn causes an enhanced depletion of Si relative to phosphate and nitrate with diatom growth and thus causes much higher Si versus P slopes in Fe-limited regions such as the Southern Ocean. If Si and Zn uptake are indeed linked, then Fe limitation may not only cause Si:P ratios to increase in diatoms but also Zn:P ratios as well, explaining the similar pattern observed in Si versus P and Zn versus P slopes in the ocean. In experiments with the coastal diatom *T. pseudonana,* silica uptake was found to be a Zn-dependent process (Rueter and Morel 1981), suggesting a causal linkage between diatom uptake of silica and zinc in seawater. Such a causal linkage between iron limitation and enhanced uptake and utilization of zinc is further supported by our experiments with *T. oceanica,* which show that iron limitation substantially increases cellular Zn:C ratios.

From the above discussion, a chain of events can be proposed that could explain the high Cd versus P slopes observed in Fe-limited regions, such as the Southern Ocean and subarctic Pacific. The initial factor is Fe limitation of the diatom growth rate, which causes both cellular Si:P and Zn:P ratios to increase. This in turn causes a steep decrease in concentrations of Zn relative to those of phosphate with diatom growth. As the Zn declines, there is a concomitant decrease in free Zn ion concentrations, which becomes accentuated as the level of dissolved Zn falls below that of the strong Zn-binding ligand. As $\log[Zn^{2+}]$ declines, there is an induction of the Cd/Co transport system that greatly increas-

es Cd uptake rates and, thus, algal Cd:P and Cd:C ratios. The high algal Cd:P ratios then result in Cd versus P relationships with very high slopes, as observed in the Fe-limited waters of the Southern Ocean. A small amount of the increase in the Cd versus P slopes could result from direct iron limitation effects on cellular cadmium content (*see Fig. 8B*), but the major influence should result from the indirect effect of zinc depletion.

The above scenario suggests direct cause and effect linkages between Fe limitation in the ocean and elevated Si:P, Zn:P, and Cd:P slopes within the nutricline. These linkages need to be considered in the use of Cd versus P relationships to model past nutrient distributions and biological drawdown of CO_2. This is particularly true since a relaxation of Fe limitation in the Southern Ocean during glacial times has been argued to have been a major factor in lowering atmospheric CO_2 concentrations and in decreasing greenhouse warming during glacial periods (Martin and Fitzwater 1988).

References

BOYLE, E. A. 1988. Cd: chemical tracer of deep-water paleooceanography. Paleooceanography **3:** 471–489

———. 1992. Oceanic chemical distributions during the stage 2 glacial maximum: Cd and δ ^{13}C evidence compared. Annu. Rev. Earth Planet. Sci. **20:** 245–287.

———, F. SCLATER, AND J. M. EDMOND. 1976. On the marine geochemistry of Cd. Nature **263:** 42–44.

BRAND, L. E., R. R. L. GUILLARD, AND L. S. MURPHY. 1981. A method for rapid and precise determination of acclimated phytoplankton reproduction rates. J. Plankton Res. **3:** 193–201.

BRULAND, K. W. 1980. Oceanographic distributions of cadmium, zinc, nickel and copper in the North Pacific. Earth Planet. Sci. Lett. **47:** 176–198.

———. 1989. Complexation of Zn by natural organic ligands in the central North Pacific. Limnol. Oceanogr. **34:** 269–285.

———. 1992. Complexation of Cd by natural organic ligands in the central North Pacific. Limnol. Oceanogr. **37:** 1008–1017.

———, AND R.P. FRANKS. 1983. Mn, Ni, Cu, Zn, and Cd in the western North Atlantic, p. 395–414. *In* C. S. Wong, E. Boyle, K. W. Bruland, J. D. Burton, and E. D. Goldberg [eds.], Trace metals in sea water. Plenum Press.

———, G. A. KNAUER, AND J. H. MARTIN. 1978. Cd in northeast Pacific waters. Limnol. Oceanogr. **23:** 618–625.

———, ———, AND ———. 1978. Zn in north-east Pacific water. Nature **271:** 741–743.

BYRNE R. H., L. R. KUMP, AND K. J. CANTRELL. 1988. The influence of temperature and pH on trace metal speciation in seawater. Mar. Chem. **25:** 163–181.

COALE, K. H., AND K. W. BRULAND. 1987. Oceanic stratified euphotic zone as elucidated by ^{234}Th:^{238}Th disequilibria. Limnol. Oceanogr. **32:** 189–200.

CULLEN, J. T., T. W. LANE, F. M. M. MOREL, AND R. M. SHERRELL. 1999. Modulation of Cd uptake in phytoplankton by seawater CO_2 concentration. Nature **402:**165–166.

DYMOND, J., AND M. LYLE. 1985. Flux comparisons between sediments and sediment traps in the eastern tropical Pacific: Implications for atmospheric CO_2 variations during the Pleistocene. Limnol. Oceanogr. **30:** 699–712.

ELDERFIELD, H., AND R. E. M. RICKABY. 2000. Oceanic Cd/P ratio and nutrient utilization in the glacial Southern Ocean. Nature **405:** 305–310.

FREW, R. D., AND K. A. HUNTER. 1992. Influence of Southern Ocean waters on the Cd-phosphate properties of the global ocean. Nature **360:** 144–146.

GUILLARD, R. R. L., AND J. H. RYTHER. 1962. Studies of marine planktonic diatoms. I. *Cyclotella nana* (Hustedt) and *Detonula Confervacea* (Cleve) Gran. Can. J. Microbiol. **8:** 229–239.

HART, B. A., P. E. BERTRAM, AND B. D. SCAIFE. 1979. Cd transport by *Chlorella pyrenoidosa.* Environ. Res. **18:** 327–335.

HUDSON, R. J. M., AND F. M. M. MOREL. 1993. Trace metal transport by marine microorganisms: implications of metal coordination kinetics. Deep-Sea Res. **40:** 129–151.

HUTCHINS, D. A., AND K. W. BRULAND. 1998. Fe-limited diatom growth rate and Si:N uptake ratios in a coastal upwelling regime. Nature **393:** 561–564.

KNAUER, G. A., AND J. H. MARTIN. 1981. Phosphorus-Cd cycling in northeast Pacific waters. J. Mar. Res. **39:** 65–76.

LANDING, W. M., AND K. W. BRULAND. 1980. Mn in the North Pacific. Earth Planet. Sci. Lett. **49:** 45–56.

LEE, J. G., AND F. M. M. MOREL. 1995. Replacement of Zn by Cd in marine phytoplankton. Mar. Ecol. Prog. Ser. **127:** 305–309.

———, S. B. ROBERTS, AND F. M. M. MOREL. 1995. Cd: A nutrient for the marine diatom *Thalassiosira weissflogii.* Limnol. Oceanogr. **40:** 1056–1063.

MARTIN, J. H., AND S. E. FITZWATER. 1988. Fe deficiency limits phytoplankton growth in the northeast Pacific subarctic. Nature **331:** 341–343.

———, ———, AND R. M. GORDON. 1990*a*. Fe deficiency limits phytoplankton growth in Antarctic waters. Global Biogeochem. Cycles **4:** 5–12.

———, R. M. GORDON, AND S. E. FITZWATER. 1990*b*. Fe in Antarctic waters. Nature **345:** 156–158.

———, ———, ———, AND W. W. BROENKOW. 1989. VERTEX: Phytoplankton/Fe studies in the Gulf of Alaska. Deep-Sea Res. **36:** 649–680.

MOREL, F. M. M., AND R. J. M. HUDSON. 1984. The geobiological cycle of trace elements in aquatic systems: Redfield revisited, p. 251–281. *In* W. Stumm [ed.]. Chemical processes in lakes. Wiley.

———, J. R. REINFELDER, S. B. ROBERTS, C. P. CHAMBERLAIN, J. G. LEE, AND D. YEE. 1994. Zn and carbon co-limitation of marine phytoplankton. Nature **369:** 740–742.

PASCIAK, W. J., AND J. GAVIS. 1974. Transport limitation of nutrient uptake in phytoplankton. Limnol. Oceanogr. **19:** 881–888.

PRICE, N. M., AND F. M. M. MOREL. 1990. Cd and Co substitution for Zn in a marine diatom. Nature **344:** 658–660.

REDFIELD, A. C., B. H. KETCHUM, AND F. A. RICHARDS. 1963. The influence of organisms on the composition of seawater, p. 26–77. *In* M. N. Hill [ed.]. The sea, v. 2. Wiley.

RUETER, J. G., AND F. M. M. MOREL. 1981. The interaction between zinc deficiency and copper toxicity as it affects the silicic acid uptake mechanisms in *Thalassiosira pseudonana.* Limnol. Oceanogr. **26:** 67–73.

SAAGAR, P. M., H. J. W. DE BAAR, AND R. J. HOWLAND. 1992. Cd, Zn, Ni, and Cu in the Indian Ocean. Deep-Sea Res. **39:** 9–35.

SUNDA, W. G. 1994. Trace metal/phytoplankton interactions in the sea, p. 213–247. *In* G. Bidoglio and W. Stumm [eds.]. Chemistry of aquatic systems: Local and global perspectives. ECSC, EEC, EAEC.

———, AND S. A. HUNTSMAN. 1986. Relationships among growth rate, cellular Mn concentrations, and Mn transport kinetics in estuarine and oceanic species of the diatom *Thalassiosira.* J. Phycol. **22:** 259–270.

———, AND ———. 1992. Feedback interactions between Zn and phytoplankton in seawater. Limnol. Oceanogr. **37:** 25–40.

———, AND ———. 1995*a*. Co and Zn interreplacement in marine phytoplankton: Biological and geochemical implications. Limnol. Oceanogr. **40:** 1404–1417.

———, AND ———. 1995*b*. Fe uptake and growth limitation in oceanic and coastal phytoplankton. Mar. Chem. **50:** 189–206.

———, AND ———. 1996. Antagonisms between Cd and Zn toxicity and Mn limitation in a coastal diatom. Limnol. Oceanogr. **41:** 373–387.

———, AND ———. 1998*a*. Control of Cd concentrations in a coastal diatom by free ionic Cd, Zn, and Mn in seawater. EnvFe. Sci. Technol. **32:** 2961–2968.

———, AND ———. 1998*b*. Interactions among Cu^{2+}, Zn^{2+}, and Mn^{2+} in controlling cellular Mn, Zn, and growth rate in the coastal alga *Chlamydomonas*. Limnol. Oceanogr. **43:** 1055–1064.

TAKEDA, S. 1998. Influence of Fe availability on the nutrient consumption ratio of diatoms in oceanic waters. Nature **393:** 774–777.

VALLEE, B. L., AND D. S. AULD. 1990. Zn coordination, function and structure of Zn enzymes and other proteins. Biochemistry **29:** 5647–5659.

Received: 13 March 2000
Accepted: 13 July 2000
Amended: 25 July 2000